THERMAL PROPERTIES OF ZINC NANOCRYSTALS: A COMPARISON STUDY USING THEORETICAL MODELS

Unal Domekeli[1], Murat Celtek[2], Sedat Sengul[1]

[1]Dept. of Physics, Trakya University, 22030, Edirne – TURKEY
[2]Faculty of Education, Trakya University, 22030, Edirne – TURKEY

Abstract

 In this study, thermal properties of zinc (Zn) nanocrystals such as melting temperature and cohesive energy depending on size were investigated with theoretical models based on thermodynamic principles. Three different nanostructures were studied as nanocrystals: 0-dimensional (nanoparticle), 1-dimensional (nanowire) and 2-dimensional (nanofilm). Two different theoretical models were used to compare the results. The obtained results show that the melting temperature and cohesive energy change depending on the size and dimension of the nanocrystal. While this change is observed radically up to ~10 nm, the rate of change decreases after ~10 nm. In addition, the variation of the melting temperature of Zn nanowire with respect to size shows that the theoretical model results are consistent when compared with the experimental results.

Keywords: Zinc, Nanocrystal, Melting point, Cohesive energy, Size effect, Dimension effect.

INTRODUCTION

 Due to the unique properties of nanocrystals depending on their size, shape and dimension, they have recently been the basis of groundbreaking developments in many fields [1,2]. They have the potential to create new materials and therefore their properties and interactions are a very popular research topic. In particular, the melting mechanism of nanocrystals is quite complex phenomena. There is still an important knowledge gap when it comes to understanding this complex mechanism, which is difficult to investigate with experimental methods. Since the first report on the size-dependent melting temperature of small particles via transmission electron microscopy [3], many melting theories based on thermodynamics have been developed on the melting process of nanocrystals [4-14]. For example, Nanda et al. [9] reported model parameters for many elements using the liquid drop model that they developed for size-dependent melting for low-dimensional systems. Although the liquid drop model has a simple form, when compared with the experimental results, it gives good results for some elements, but fails to explain the size-

dependent change of melting for many elements. In addition, the liquid drop model has not been developed for one-component systems. Lu et al. [12] developed a new model based on thermodynamic quantities and investigated the size-dependent thermodynamic properties of pure gold, silver, nickel, argon, silicon, lead and indium nanocrystals. They reported that their model produces results consistent with existing experimental and molecular dynamics (MD) simulation results. Li et al. [13] estimated the melting temperature depending on size of one-component indium, tin, nickel, lead, palladium, gold and zinc and two-component Pd-Cu, Pd-Rh, and Pd-Pt nanowires by using the theoretical model that they developed based on surface area, packing factor and cross-sectional shape of the wire. The results obtained with this model showed that the melting temperatures for both one-component and two-component nanowires are consistent with the existing experimental and MD results.

 In this study, we calculated the cohesive energy and melting points of Zn nanocrystals using these size-dependent melting models developed for low structure systems. Three different nanostructures were studied as

538

nanocrystals: 0-dimensional (nanoparticle), 1-dimensional (nanowire) and 2-dimensional (nanofilm).

EXPOSITION

In this study, the theoretical models developed by Lu et al. [12] and Li et al. [13] are called as MODEL-1 and MODEL-2, respectively. MODEL-1 and MODEL-2 are models that predict a linear relationship between melting temperature and bonding energy based on the Lindemann melting criterion. In these models, when the structures of the nanocrystal and the bulk system are the same, this relationship can be expressed as follows [12,13];

$$\frac{T_m(D)}{T_{mb}} = \frac{E_c(D)}{E_{cb}} \qquad (1)$$

where $T_m(D)$ and T_{mb} are the melting temperatures of the nanocrystal and bulk system, respectively. $E_c(D)$ and E_{cb} are the cohesive energies of the nanocrystal and bulk system, respectively.

According to MODEL-1, size, shape and dimension effects on the ratio of surface atoms to all atoms are combined and the melting temperature and cohesive energy of the nanocrystal are given as follows [12], respectively;

$$T_m(D) = T_{mb}\left[\left(1 - \frac{1}{12D_o - 1}\right) \times \right. \qquad (2)$$

$$\left. exp\left(-\frac{2\lambda S_{bo}}{3R}\frac{1}{12D_o - 1}\right)\right]$$

$$E_c(D) = E_{cb}\left[\left(1 - \frac{1}{12D_o - 1}\right) \times \right. \qquad (3)$$

$$\left. exp\left(-\frac{2\lambda S_{bo}}{3R}\frac{1}{12D_o - 1}\right)\right]$$

where D is the size of the nanocrystal, representing the diameter for the spherical nanoparticle (NP) and the cylindrical nanowire (NW), and the film thickness for the nanofilm (NF). R is the ideal gas constant and D_o is a critical size where all atoms of the crystal are located on its surface and can be determined as [12]:

$$D_o = 2(3 - d)h \qquad (3)$$

i)   for d=0 spherical NPs $D_o = 6h$,
ii) for d=1 cylindrical NWs $D_o = 4h$,
iii) for d=2 NFs $D_o = 2h$

where h is the distance between atoms. $S_{bo} = \Delta H_{bo}/T_{bo}$ is the bulk solid-vapor transition entropy. H_{bo} and T_{bo} are the bulk enthalpy of vaporization and the bulk boiling point, respectively. λ is the shape factor of the nanocrystal and is determined from the ratio of the number of the surface atoms to the total number of atoms ($\lambda = 1$ for spherical NP, cylindrical NW and NF [12]). The parameters used in MODEL-1 calculations for Zn are given in Table 1.

Table 1. MODEL-1 parameters for Zn

metal	parameters				
	$T_{mb}(K)$	$T_{bo}(K)$	$E_{cb}(eV)$	$\Delta H_{bo}(kJ/mol)$	$h(nm)$
Zn	692.7[a]	1180[b]	-1.35[a]	119[b]	0.267[b]

[a] Ref. [15]
[b] Ref. [16]

According to MODEL-2 based on surface area, packing factor and cross-sectional shape of nanocrystal, the melting temperature and cohesive energies for spherical NP, cylindrical NW and NF can be calculated from the expressions given below, respectively [13];

$$T_{mnp}(D) = T_{mb}\left[1 - \frac{2P_s}{\frac{fD}{d} + 2P_s}\right] \qquad (4)$$

$$E_{cnp}(D) = E_{cb}\left[1 - \frac{2P_s}{\frac{fD}{d} + 2P_s}\right] \qquad (5)$$

$$T_{mnw}(D) = T_{mb}\left[1 - \frac{2P_s}{\frac{3fD}{2d} + 2P_s}\right] \qquad (6)$$

$$E_{cnw}(D) = E_{cb}\left[1 - \frac{2P_s}{\frac{3fD}{2d} + 2P_s}\right] \qquad (7)$$

$$T_{mnf}(D) = T_{mb}\left[1 - \frac{P_s}{\frac{3fD}{d2} + P_s}\right] \qquad (8)$$

$$E_{cnf}(D) = E_{cb}\left[1 - \frac{P_s}{\frac{3fD}{d2} + P_s}\right] \qquad (9)$$

where P_s and f are the packing fraction of the surface crystal plane and packing factor, respectively. The parameters used in MODEL-2 calculations for Zn are given in Table 2.

Table 2. MODEL-2 parameters for Zn

metal	parameters				
	$T_{mb}(K)$	$E_{cb}(eV)$	$d(nm)$	P_s	f
Zn	692.7[a]	-1.35[a]	0.282[a]	0.91[b]	0.74[b]

[a] Ref. [15]
[b] Ref. [13]

For Zn nanocrystals, the size-dependent variations of the melting temperature and cohesive energy calculated using MODEL-1 and MODEL-2 are given in Figures 1 and 2, respectively. As can be seen from Figure 1a-c, the melting temperatures obtained from both MODEL-1 and MODEL-2 for spherical NP, cylindrical NW and NF are smaller than that of the bulk Zn. For both models, the melting temperature increases as the size of the nanocrystal increases. While the rate of increase observed in the melting temperature occurs dramatically up to about $D = \sim10$ nm, after $D = \sim10$ nm the rate of increase gradually decreases with increasing size. As the size of the NP decreases, the surface/volume atomic ratio increases. For example, for a NP with the diameter of $D = \sim10$ nm, the surface atoms occupy 25% of the total atomic number, whereas for a ~100 and ~1000 nm diameter NP this ratio is only 2.5% and 0.25%, respectively [13]. Therefore, the smaller the size of the NP, the more dominant the influence of the surface atoms in the system. This explains their influence on the physical and chemical properties of NP. As the size of the NP decreases, the surface effects become more pronounced on the thermodynamic properties. As the size increases, this effect gradually
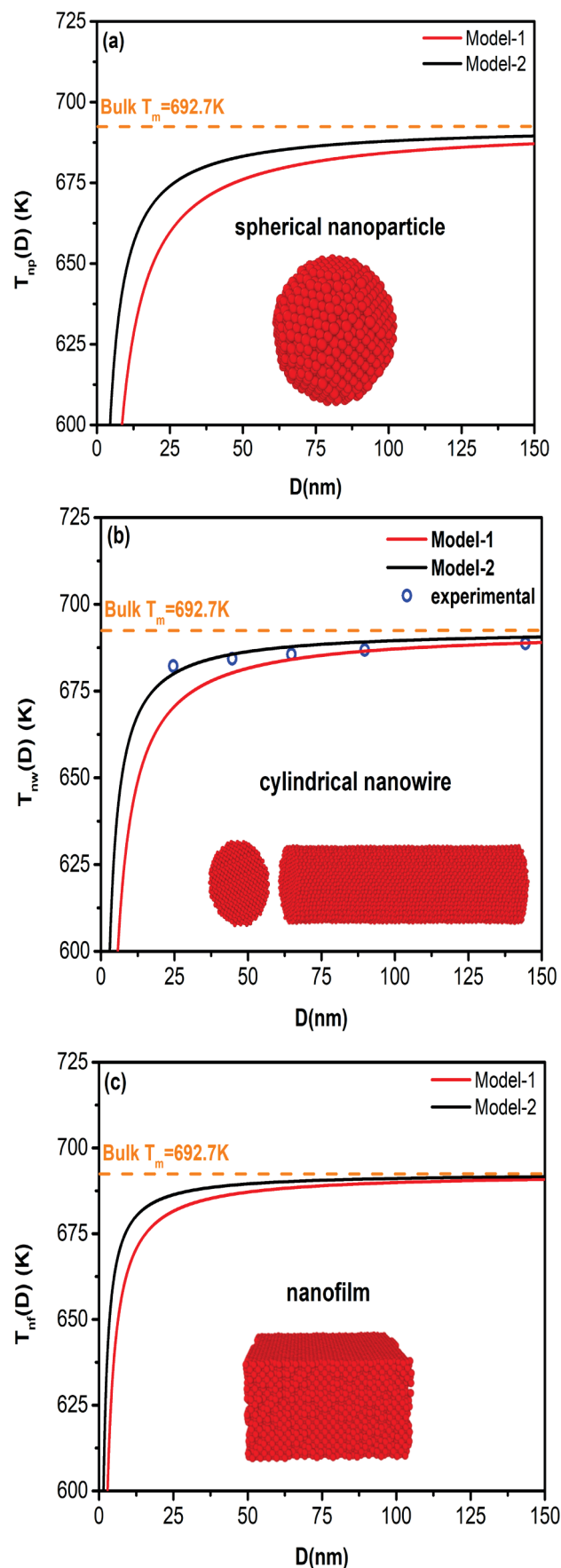

Fig. 1. Variation of the melting temperatures of Zn (a) NP, (b) NW and (c) NF depending on the size.
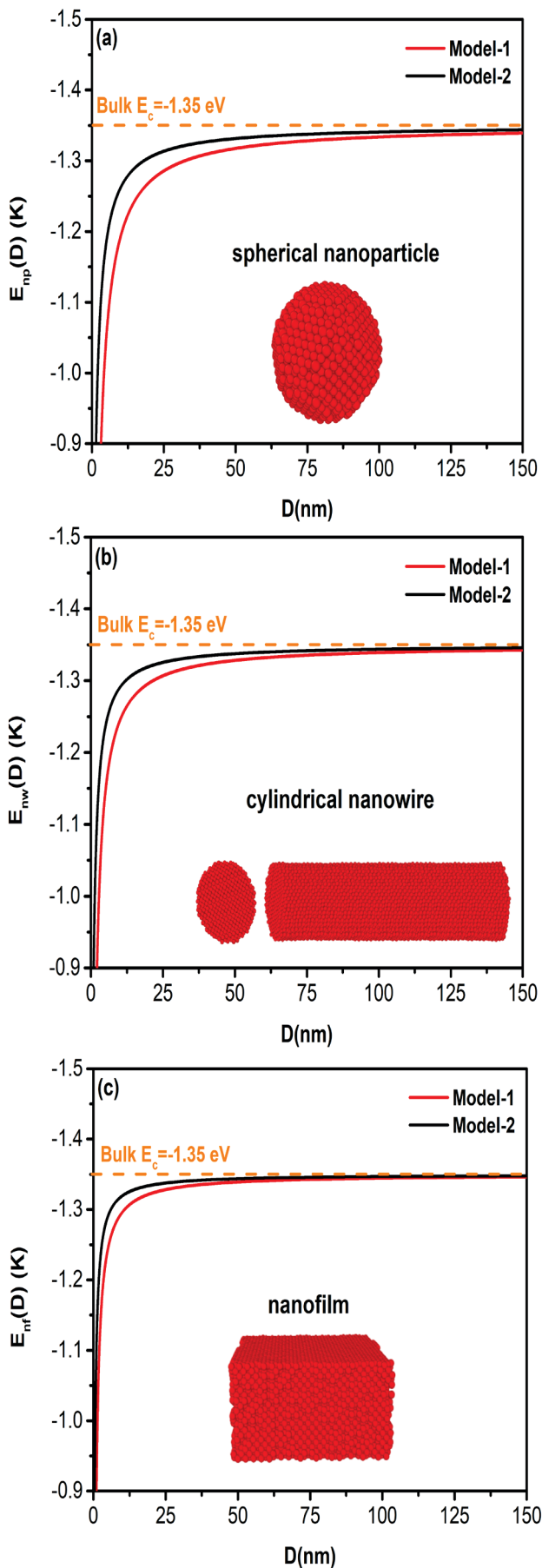
Fig. 2. *Variation of the cohesive energies of Zn (a) NP, (b) NW and (c) NF depending on the size.*

decreases. This is also valid for the cases in NW and NF. As can be seen from Figure 1b, the melting temperatures obtained from both models for NW are consistent with the experimental results. Especially when the diameter of the cylindrical wire is smaller than $D = \sim 50$ nm, the MODEL-2 results show a better agreement with the experimental results, while the MODEL-1 results are in better agreement with the experimental results for the diameter values larger than $D = \sim 50$ nm. In addition, the melting temperatures obtained from MODEL-2 for each nanocrystal structure are larger compared to MODEL-1. For example, for NP with a diameter of ~ 10 nm, the melting temperatures obtained from MODEL-1 and MODEL-2 are 612 K and 648 K, respectively. As can be seen from Figure 2 a-c, the cohesive energies calculated from both models decrease with increasing the size of the nanocrystal. At large size values, the cohesive energy of nanocrystals converges to the value of the bulk Zn. At small size values, the cohesive energy of nanocrystals is greater than that of the bulk. Nanocrystals with low coordination number of atoms on the surface have high surface energy and therefore higher cohesive energy than the bulk materials. This indicates that the nanocrystal is more unstable compared to the bulk material. As the size of the nanocrystal increases, the surface/volume atoms ratio decreases, so the surface effects begin to weaken, and the cohesive energy of the nanocrystal converges towards the bulk value. Also, the cohesive energies obtained from MODEL-2 for NP are smaller than those calculated from MODEL-1. For example, for NP with a diameter of ~ 10 nm, the cohesive energies obtained from MODEL-1 and MODEL-2 are -1.19 eV and -1.26 eV, respectively. The behaviors of the size-dependent variation of melting and cohesive energies of NW and NF are similar to that of NP.

Figure 3 shows the variation of melting temperatures and cohesive energies calculated from MODEL-1 depending on the dimension of the nanocrystal. The melting temperature changes depending on the dimension of nanocrystal. It is seen that the melting temperatures calculated from MODEL-1 for NP, NW and NF increase with increasing size.
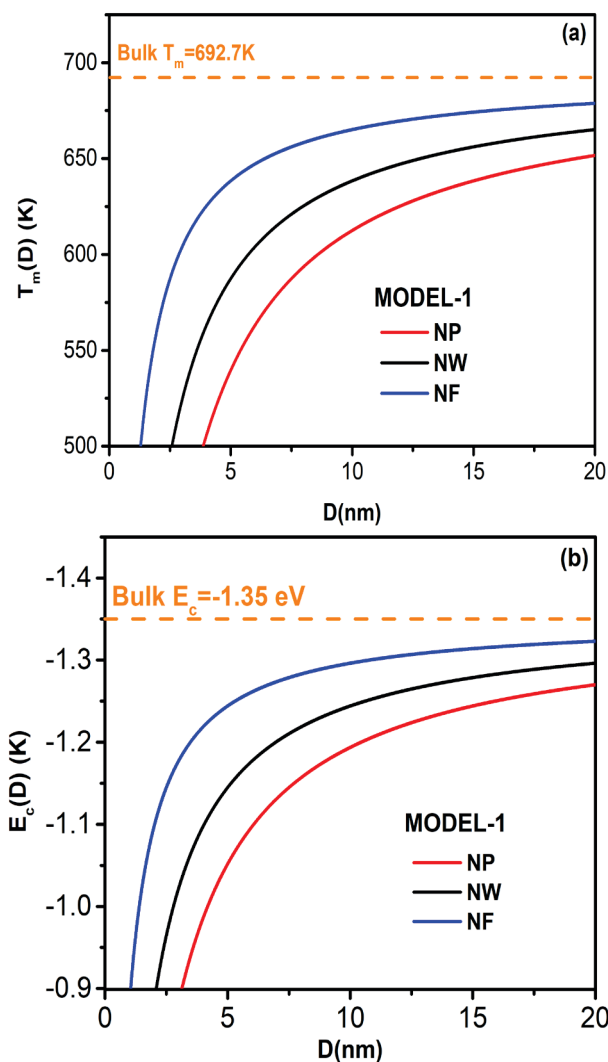
541

Fig. 3. *Variation of (a) the melting temperatures and (b) the cohesive energies of Zn nanocrystal depending on the dimension for MODEL-1.*

Fig. 4. *Variation of (a) the melting temperatures and (b) the cohesive energies of Zn nanocrystal depending on the dimension for MODEL-2.*

For example, for the $D = \sim 10$ nm, the melting temperatures of NP, NW, and NF are 612 K, 638 K, and 667 K, respectively. The melting temperature is greatest for NF and smallest for NP. When the cohesive energies calculated from MODEL-1 for NP, NW and NF are compared with each other, NP has the largest cohesive energy, while NF has the smallest cohesive energy. For example, for $D = \sim 10$ nm, the cohesive energies of NP, NW and NF are -1.19 eV, -1.24 eV and -1.30 eV, respectively.

The behavior of the melting temperature and cohesive energy calculated from MODEL-2 depending on the size of nanocrystal is given in Figure 4. The results obtained from MODEL-2 exhibit similar characteristic behaviors with the results of MODEL-1. These results show that the melting temperature and cohesive energy depend dramatically on the dimensionalas well as the size of the nanocrystal.
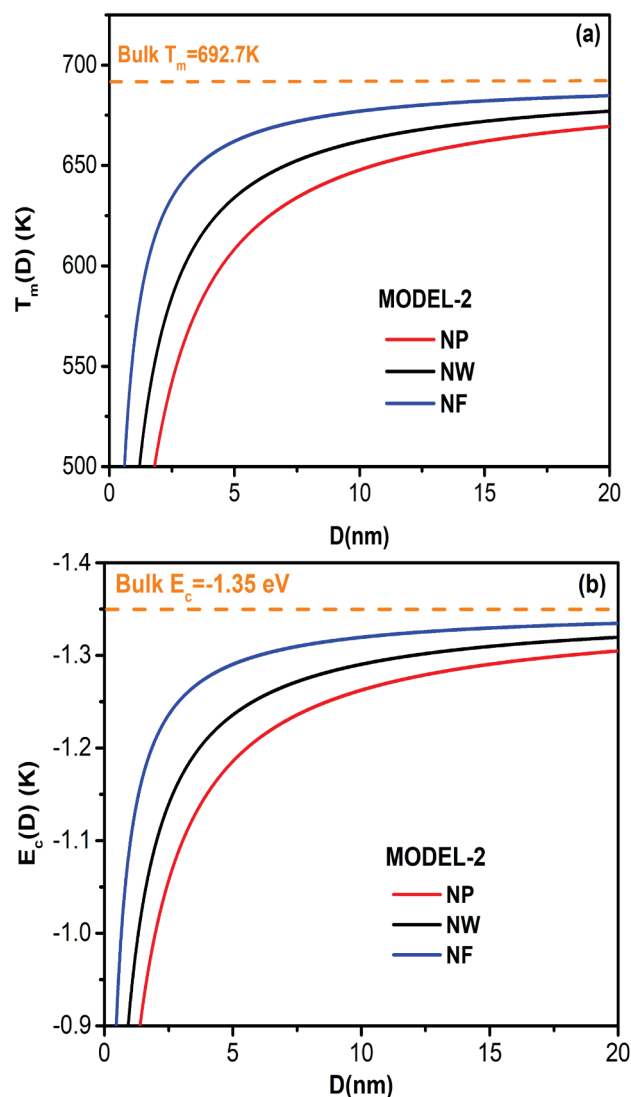
CONCLUSION

In this study, we performed a comparison of MODEL-1 and MODEL-2, which are used to describe the size, shape and dimensionality dependencies of cohesive energy and melting temperature of Zn nanocrysals. The obtained results show that the cohesive energy and melting temperature vary depending on the size and dimensionality of the nanocrystal. For both models, as the size of the nanocrystal increases, the melting temperature increases and the cohesive energy decreases. As the size of nanocrystal gets smaller, the surface/volume atom ratio increases and surface effects become dominant in the system. This increases the surface energy of the nanocrystal, resulting in an increase in the cohesive energy. Due to these surface

542

effects, the nanocrystal melts at a lower temperature than the melting temperature of the bulk, performing a surface melting. The melting temperatures calculated from both models for Zn NW are consistent with the experimental values. The results of the MODEL-1 in large sizes and the results of the MODEL-2 in small sizes show a good agreement with the experimental results. These models can also be applied to investigate the melting temperature and cohesive energy of different low-dimensional systems, as their predictions for the melting temperature are consistent with the experimental results.

REFERENCE

[1] D. Pullini, G. Innocenti, D. Busquets, A. Ruotolo, Appl. Phys. Lett., 90, 133106 (2007).

[2] J. Zhang, K. Sasaki, E. Sutter, R.R. Adzic, Science 315, 220 (2007).

[3] M. Takagi, J. Phys. Soc. Jpn. 9, 359 (1954).

[4] J. Shanker, M. Kumar, Phys. Stat. Solidi B 158, 11 (1990).

[5] R. R. Couchman, Philos. Mag. A 40, 637 (1979).

[6] R. R. Vanfleet and J. M. Mochel, Surf. Sci. 341, 40 (1995).

[7] Q. Jiang, L. H. Liang and J. C. Li, J. Phys.: Condens. Matt. 13, 565 (2001).

[8] C. Q. Sun, Y. Wang, B. K. Tay, S. Li, H. Huang and Y. B. Zhang, J. Phys. Chem. B 106, 10701 (2002).

[9] K. K. Nanda, S. N. Sahu and S. N. Behera, Phys. Rev. A 66, 013208 (2002).

[9] W. H. Qi, M. P. Wang, M. Zhou and W. Y. Hu, J. Phys. D: Appl. Phys. 38, 1429 (2005).

[10] W. H. Qi, M. P. Wang, M. Zhou, X. Q. Shen and X. F. Zhang, J. Phys. Chem. Sol. 67, 851 (2006).

[11] A. Safaei, M. A. Shandiz, S. Sanjabi and Z. H. Barber, J. Phys.: Condens. Matter 19, 216216 (2007).

[12] H. M. Lu, P. Y. Li, Z. H. Cao and X. K. Meng, J. Phys. Chem. C 113, 7598 (2009).

[13] Y. J. Li, W. H. Qi, B. Y. Huang, M. P. Wang and S. Y. Xiong, Modern Phys. Lett. B, 24 (22), 2345–2356 (2010).

[14] S. Bhatt, M. Kumar, J. Phys. and Chem. Solid. 106, 112–117 (2017).

[15] Kittel C. Introduction to Solid State Physics. New York: John Wiley & Sons Inc., 1986.

[16] http://www.webelements.com/.